

The simultaneous quantification of cytochrome P450 dependent linoleate and arachidonate metabolites in urine by HPLC-MS/MS

John W. Newman, Takaho Watanabe, and Bruce D. Hammock¹

Department of Entomology and the UC Davis Cancer Center, University of California, Davis, CA

Abstract A method for the simultaneous quantification of urinary linoleic and arachidonic acid derived epoxides and diols, as well as the arachidonate omega hydroxylated product has been developed. The method employs negative mode electrospray ionization and HPLC with tandem mass spectroscopy for quantification. Odd chain length saturated epoxy and dihydroxy fatty acids are used as analytical surrogates resulting in linear calibrations ($r^2 \geq 0.9995$). Standard addition analyses showed that matrix effects do not prevent these surrogates from yielding reliable quantitative results. Using 4 ml urine aliquots at a final extract volume of 100 μ l and injecting 10 μ l, method detection limits and limits of quantification were ≤ 0.5 and 1.5 nM, respectively. The sensitivity for dihydroxy lipids was from 3- to 10-fold greater than the corresponding epoxy fatty acid. Shot to shot run times of 31 min were achieved. Rodent and human urine analyses indicated the method sensitivity is sufficient for general research applications. In addition, diurnal fluctuations in linoleate and arachidonate derived metabolites were observed in human subjects.—Newman, J. W., T. Watanabe, and B. D. Hammock. The simultaneous quantification of cytochrome P450 dependent linoleate and arachidonate metabolites in urine by HPLC-MS/MS. *J. Lipid. Res.* 2002, 43: 1563–1578.

Supplementary key words epoxy fatty acids • epoxyeicosatrienoic acid • dihydroxyeicosatrienoic acid • 20-hydroxyeicosatetraenoic acid • leukotoxin • soluble epoxide hydrolase • electrospray ionization

Cytochrome P450s (CYPs) produce a number of oxidized fatty acids, including epoxy and monohydroxy metabolites (1–4). Polyunsaturated epoxides can also be formed by the rearrangement of lipid hydroperoxides (5–7). These chemically stable epoxides are further metabolized to their corresponding vicinal diols by the soluble epoxide hydrolase (8, 9). The hydroxylated lipids can be further transformed into glucuronides (10, 11), and possibly other conjugates, prior to excretion. Many lipid oxidation products, including products of CYP metabolism,

have been reported in mammalian urine (10–14). As has been the case for prostanoids and thromboxanes (15–17), the quantification of CYP derived oxylipids in urine will likely provide insight into the activity of this biochemical cascade, as well as the physiological state of the subject.

The enzymatic oxidation of arachidonic acid is a key factor in the blood pressure regulatory cascade (2, 18). Hydroxylation of the ω -carbon of the arachidonic acid chain yields 20-hydroxy eicosatetraenoic acid (20-HETE), a potent vasoconstrictor (2). The 20-HETE inhibits large and medium conductance calcium dependent potassium (K^+_{Ca}) channels (19), preventing cellular hyperpolarization. This action of 20-HETE is opposed by the epoxides of arachidonic acid, i.e. epoxy eicosatrienoic acids (EETs), which increase the open state probability of K^+_{Ca} channels (3, 20, 21). In particular, the 11(12)-EET has been suggested as an endothelial derived hyperpolarization factor (20, 22). The EET regioisomers also affect mitogenesis and hormone secretion (1). Complicating matters, the specificity of regioisomeric activity varies between cell type and vascular bed (2). The 14,15-, 11,12-, and 8,9-EETs are excellent substrates for the soluble epoxide hydrolase (sEH). The sEH transforms the epoxides into their corresponding dihydroxy eicosatrienoic acids or dihydroxyeicosatrienoic acids (DiHETs) (23). The 5,6-EET is hydrated slowly by sEH (23). While the DiHETs have vasodilatory actions in canine coronary arterioles (24), the introduc-

Abbreviations: BHT, butylated hydroxy toluene; CYP, cytochrome P450; DiHET, dihydroxyeicosatrienoic acid; DiHOME, dihydroxyoctadecenoic acid; DiHN, dihydroxynonadecanoic acid; ϵ , molar extinction coefficient; EET, epoxyeicosatrienoic acid; EpHep, epoxyheptadecanoic acid; EpOME, epoxyoctadecenoic acid; 20-HE, 20-hydroxyeicosanoic acid; 20-HETE, 20-hydroxyeicosatetraenoic acid; IDL, instrumental detection limit; ISTD, internal standard; IUPAC, International Union of Pure and Applied Chemistry; K^+_{Ca} , calcium-dependent potassium; LOQ, limit of quantification; $[M-H]^-$, deprotonated molecular ion; MDL, method detection limit; MS, mass spectroscopy; MS/MS, tandem quadrupole mass spectroscopy; SD, Sprague-Dawley rat; sEH, soluble epoxide hydrolase; SHR, spontaneously hypertensive rat; TPP, triphenyl phosphine; S:N, signal to noise ratio; SSTD, surrogate standard.

¹ To whom correspondence should be addressed.

e-mail: bdhammock@ucdavis.edu

Manuscript received 23 April 2002.

DOI 10.1194/jlr.D200018-JLR200

Copyright © 2002 by Lipid Research, Inc.

This article is available online at <http://www.jlr.org>

tion of free hydroxyl moieties inhibits their incorporation into membranes (25) and promotes their elimination as glucuronide conjugates in humans (11, 26, 27). In contrast, hydroxy lipid glucuronidation appears to be deficient in rats, and the hydroxyl lipids are eliminated directly (28). While receiving less attention, linoleate derived dihydroxy lipids are also bioactive. These octadecanoid diols or dihydroxyoctadecenoic acids (DiHOMEs) inhibit mitochondrial respiration (8, 29, 30), increase vascular permeability (31), and have been identified as their glucuronide conjugates in the urine of children with generalized peroxisomal disorders (10). Therefore, the simultaneous determination of both linoleate and arachidonate derived oxidation products in urine may provide unique insights into the associations between these compounds under various physiological conditions, including disease.

The following study was conducted with two primary goals. First, to establish a simple and sensitive analytical method for the simultaneous detection of the EETs, DiHETs, and 20-HETE, along with the linoleate derived epoxides and diols in urine. The second goal was to provide a preliminary assessment of baseline excretion profiles of these oxidized lipids in apparently healthy humans.

MATERIALS AND METHODS

Chemical nomenclature

The International Union of Pure and Applied Chemistry (IUPAC) has adopted the abbreviations for oxidized fatty acids following the recommendations of Smith et al. (32, 33) as shown in

Table 1 and **Table 2**. In short, for unsaturated epoxy fatty acids, abbreviations indicate epoxide position, chain length, and degrees of unsaturation. Therefore, 14(15)-epoxyeicostri-(5Z,8Z,11Z)-enoic acid is reduced to 14(15)-EpETrE while 9(10)-epoxyoctadec-(12Z)-enoic acid becomes 9(10)-epoxyoctadecenoic acid (EpOME). Dihydroxy lipids are named similarly, such that 14,15-dihydroxyeicostri-(5Z,8Z,11Z)-enoic acid becomes 14,15-DiHETrE, while 20-hydroxyeicosatetra-(5Z,8Z,11Z,14Z)-enoic acid is 20-HETE. The EpETrEs and DiHETrEs are more commonly known as EETs and DiHETs, respectively. The common abbreviations are used throughout the text to improve the readability of the manuscript.

Chemicals

Unsaturated lipids were purchased from NuChek Prep (Elysian, MN). Purified DiHET regioisomers synthesized in the laboratory of Dr. J. R. "Camille" Falck were a kind gift from Dr. Darryl C. Zeldin at the National Institute of Environmental Health Sciences (Research Triangle Park, NC). The 20-HETE and 5(6)-EET were purchased from Cayman Chemical (Ann Arbor, MI). The 20-hydroxy eicosanoic acid (20-HE) was purchased from Larodan Fine Chemicals (Malmö, Sweden). Hexane, ethyl acetate, chloroform, and glacial acetic acid of HPLC Grade or better were purchased from Fisher Scientific (Pittsburgh, PA). OmniSolv™ acetonitrile and methanol purchased from EM Science (Gibbstown, NJ) was used for all reverse phase HPLC analyses. All other chemical reagents were purchased from either Sigma (St. Louis, MO) or Aldrich Chemical Co (Milwaukee, WI) unless indicated.

Instrumentation

Purification of epoxy lipids was accomplished on an HP1100 series HPLC with a HP1050 diode array detector (Agilent Technologies; San Jose, CA). Preparative scale isolations used a 22.5 × 250 mm, 5 μm ODS(2) Spherclone column (Phenomenex, Torrance, CA). Analytical scale analysis with diode array detec-

TABLE 1. Optimized collision voltages and transition ions for epoxy fatty acids

Analyte ^a	CV ^b	Transition ^c	Molecular and Transition Ion Structure(s)
10(11)-EpHep	-20	283 > 265 (82%) ^d 283 > 185 (42%)	
12(13)-EpOME [isoleukotoxin]	-17	295 > 195 (27%) ^d	
9(10)-EpOME [leukotoxin]	-17	295 > 171 (63%) ^d	
14(15)-EpETrE [14,15-EET]	-13	319 > 219 (20%) ^d	
11(12)-EpETrE [11,12-EET]	-13	319 > 167 (41%) 319 > 208 (12%) ^d	
8(9)-EpETrE [8,9-EET]	-13	319 > 167 (17%) 319 > 155 (11%) ^d 319 > 127 (7%)	
5(6)-EpETrE [5,6-EET]	-10	319 > 191 (28%) ^d 319 > 115 (2%)	

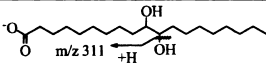
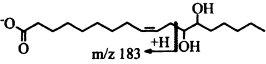
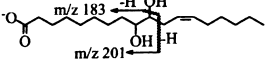
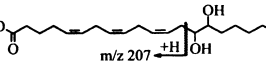
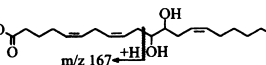
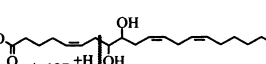
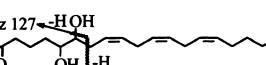
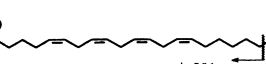
^a The International Union of Pure and Applied Chemistry (IUPAC) accepted abbreviation of oxylipids with common abbreviation in brackets.

^b Optimal collision voltage in volts with 2.3×10^{-3} Torr argon in the collision cell.

^c Characteristic mass transitions: [M-H]⁻ > [Fragment]⁻ (Fragment intensity as a percentage of the most abundant ion generated at the optimal voltage). Fragmentation was generally consistent with that reported by Nakamura et al. (53).

^d Mass transition selected for quantification.

TABLE 2. Optimized collision voltages and transition ions for hydroxy fatty acids

Analyte ^a	CV ^b	Transition ^c	Molecular and Transition Ion Structure(s)
10,11-DiHN	-26	329 > 311 (62%) ^d	
12,13-DiHOME [isoleukotoxin diol]	-20	313 > 183 (60%) ^d	
9,10-DiHOME [leukotoxin diol]	-20	313 > 201 (100%) ^d 313 > 183 (10%)	
14,15-DiHETrE [14,15-DiHET]	-17	337 > 207 (100%) ^d	
11,12-DiHETrE [11,12-DiHET]	-20	337 > 167 (100%) ^d	
8,9-DiHETrE [8,9-DiHET]	-20	337 > 127 (100%) ^d	
5,6-DiHETrE [5,6-DiHET]	-17	337 > 145 (40%) ^d 337 > 127 (5%)	
20-HETE	-15	319 > 301 (30%) ^d	

^a The IUPAC accepted abbreviation of oxylipids with common abbreviation in brackets.

^b The optimal collision voltage in volts with a collision cell pressure of 2.3×10^{-3} Torr argon.

^c Characteristic mass transitions: $[M-H]^- > [Fragment]^-$ (Fragment intensity as a percentage of the most abundant ion generated at the optimal voltage).

^d Mass transition selected for quantification.

tion was performed on a 4.6×250 mm, $5 \mu\text{m}$ ODS(2) PhaseSep analytical HPLC column (Waters, Milford, MA). GC/mass spectroscopy (MS) based confirmation was accomplished using a HP6890 gas chromatograph equipped with a $30 \text{ m} \times 0.25$ mm i.d., $0.25 \mu\text{m}$ DB-17HT (Agilent Technologies) interfaced with an HP5973 mass spectral detector.

The quantification of lipid oxidation products was performed by negative mode electrospray ionization with tandem quadrupole mass spectroscopy (MS/MS). All HPLC/MS analyses were performed with a Waters 2790 separation module equipped with a 2.0×150 mm, $5 \mu\text{m}$ Luna C18(2) column (Phenomenex) held at 20°C . The sample chamber was held at 10°C . A 75 cm segment of 0.005 inch i.d. PEEK tubing interfaced the HPLC to the electrospray ionization probe of a Quattro Ultima tandem-quadrupole mass spectrometer (Micromass, Manchester, UK). Solvent flow rates were fixed at $350 \mu\text{l}/\text{min}$ with a cone gas flow of $125 \text{ l}/\text{h}$, desolvation gas flow of $650 \text{ l}/\text{h}$, a source temperature of 125°C , and a desolvation temperature of 400°C . Electrospray ionization was accomplished in the negative mode with a capillary voltage fixed at -3.0 kV. For MS/MS experiments, argon was used as the collision gas at a pressure of 2.3×10^{-3} Torr while quadrupole mass resolution settings were fixed at 12.0 (i.e., ~ 1.5 Da resolution). The photo multiplier voltage was 650 V. Optimal cone voltage and collision voltages were established experimentally. Ion dwell times of 0.45 s were used.

HPLC solvents

A single solvent system was used for all preparative to analytical scale HPLC analyses described in this manuscript. The applied solvents were modified from Kiss et al. (34): Solvent A = 51:40:9 acetonitrile-water-methanol (v/v/v) with 0.1% glacial

acetic acid; Solvent B = 85:15 acetonitrile-methanol (v/v) with 0.1% glacial acetic acid.

Animals

Sprague-Dawley rats (SDs) and 13-week-old spontaneously hypertensive rats (SHRs) were obtained from Charles River Laboratories (Wilmington, MA) and housed in metabolic chambers with free access to food and water. All animal handling was performed in accordance with approved animal use protocols. Urine from SD rats was provided by Dr. John Imig at the Medical College of Georgia (Augusta, GA).

Oxylipid synthesis

Epoxy fatty acid methyl esters were synthesized using dimethyl dioxirane (mono-unsaturated free acids) or meta-chloro perbenzoic acid (polyunsaturated methyl esters) and purified as previously described (8, 35–37). Purified epoxides were chemically hydrolyzed to dihydroxy lipid methyl esters using 1:1 acetonitrile-aqueous 5% perchloric acid (v/v) (8, 35–37). Methyl esters were transformed to free fatty acids using published procedures (38). Briefly, methyl esters were dissolved at $10 \text{ mg}/\text{ml}$ in methanol and chilled to 0°C . While stirring, the chilled solution was enriched by the dropwise addition of $335 \mu\text{l}$ of 0.33 N sodium hydroxide per ml of ester solution. The reaction was maintained at room temperature for 12–20 h. Upon completion, the reaction was diluted with $750 \mu\text{l}$ of water per ml of reaction. The mixture was brought to pH 4.25 with $220 \mu\text{l}$ 0.25 M oxalic acid (per ml of reaction solution) and extracted four times with ethyl acetate. The extract was washed with water until the pH of the wash was unchanged. The organic fraction was dried with ~ 1 g of hexane washed anhydrous sodium sulfate and the residual solvent was removed by rotary evaporation. The progress of the reactions was

screened by spotting ~10 µl of the mixture on a 10 cm silica gel TLC plate (EM Science). The TLC plate was developed in 80:20 hexane-ethyl acetate (v/v) and visualized with heat after spraying with 4% phosphomolybdic acid in 20% ethanolic water. In the case of the EETs, 100 mg of the methyl ester was hydrolyzed in 16 h. The resulting straw colored oil was purified by loading onto 2 g of silica gel (Baker 60/40 mesh) in a 15 ml sintered glass funnel and washing with 50 ml of pentane, 20 ml of 10% ethyl acetate in pentane and 20 ml of ethyl acetate. The final ethyl acetate fraction yielded 70 mg of colorless oil (197 µmol, 70% yield). Similar yields were achieved with EpOMEs and DiHOMEs.

Abundance and purification of isomeric mixtures

The isomeric abundance of the linoleate derived epoxide mixture was quantitatively characterized. A 10 mg aliquot of the silica gel purified reaction mixture was dissolved in 1 ml of methanol. A 10 µl aliquot of this solution was diluted to 500 pg/µl, spiked with the internal standards described below, methylated, thiolated, silylated, and analyzed by GC/MS as previously described (37). An aliquot of the epoxide mixture was hydrolyzed as described above to produce diols. The resulting diols were purified by silica gel column chromatography and quantified as trimethyl silyl-ether/methyl esters by GC/MS (37).

Epoxyeicosanoid regioisomers were purified using reverse phase HPLC. A total of 70 mg of the epoxy fatty acid mixture (~10 mg/injection) were introduced to a preparative column (see Instrumentation) and separated at a flow rate of 10 mL/min (0–35 min, 70% Solvent A; 45 to 55 min, 100% Solvent B), while recording absorbance at 210 and 232 nm. Traces of 232 nm dense compounds, presumably peroxides, were observed eluting before 10 min. Epoxide isomer identity was initially assigned based on relative retention times reported in the literature (34): 14(15)-EET = 25.6 min, 11(12)-EET = 28.8 min, 8(9)-EET = 30.3 min, 5(6)-EET = 34.5 min). Peak heights showed 14(15) > 11(12) > 8(9) >> 5(6)-EET. The 5(6)-EET fatty acid purification was not attempted. The 14(15)-EET appeared fully resolved and was collected directly. The 11(12)- and 8(9)-isomers showed ~60% baseline resolution. Therefore, these peaks were collected from leading edge to 50% of the height after the apex and from the apex to the trailing edge, respectively. The collected central fractions were combined, re-purified and appropriate fractions combined. The combined HPLC fractions were extracted three times with an equal volume of pentane and the solvent was removed by vacuum rotary evaporation. The residues were re-dissolved in chloroform, transferred to storage vials, and reduced to a constant mass under a gentle stream of nitrogen at 40°C. Each fraction was then diluted and ~50 µg was reanalyzed with an isocratic solvent flow of 96% Solvent A and 4% Solvent B at 2 ml/min on the described analytical column (see Instrumentation). This solvent system gave optimal EET isomer resolution: peak widths = 0.35 min, 14(15)-EET (12.5 min), 11(12)-EET (14.3 min), and 8(9)-EET (14.7 min). The 11(12)-EET isolated under these conditions was pure (20 mg, >98% UV, 205 nm Abs). However, the 14(15)-isomer showed 13% of a late eluting unknown impurity and the 8(9)-EET was contaminated with ~10% 11(12)-EET. The impure fractions were re-purified using the preparative system but injected masses were kept below 5 mg, resulting in the isolation of 14(15)-EET (18 mg) and 8(9)-EET (6 mg) with a final purity of >98% as determined by UV absorbance at 205 nm. Full scan (195–600 nm) diode array spectra revealed no detectable secondary peaks. Methylation, thiolation, and silylation of the purified EETs followed by GC/MS analysis (37) confirmed isomer identification and indicated that the purified materials contained less than 0.5% DiHETs. The final purified fractions were concentrated and transferred as described above. The lipids were stored under nitrogen at –32°C until use.

These materials were used for the generation of all EET calibration solutions.

Surrogates, internal standards, and calibration solutions

Odd chain length monounsaturated fatty acids were used to prepare epoxide and diol extraction surrogates. Specifically, 10(11)-epoxyheptadecanoic acid [10(11)-EpHep] and 10,11-dihydroynonadecanoic acid (10,11-DiHN) were synthesized as described above. Eight independent calibration solutions containing ~1 pmol/µl of each internal standard were prepared in acetonitrile. The six lowest concentrations ranged from ~5–1,500 fmol/µl (nM). These standards contained all EpOME, DiHOME, EET, and DiHET isomers along with 20-HETE. The two additional standards extended the calibration for the EpOMEs and DiHOMEs to 25 µM and the EETs, except for the 5(6)-isomer, to 10 µM. These calibration solutions were sub-aliquoted into Wheaton pre-scored gold-band amber ampoules (Fisher Scientific), sealed under nitrogen and stored at ≤–32°C.

Optimization of MS and MS/MS Parameters

The intensity of the deprotonated molecular ion was evaluated at cone voltages between –40 V and –120 V. Initially, calibration solutions were introduced directly into the mass spectrometer with a 1:1 mixture of Solvent A and Solvent B. A secondary analyses was performed with chromatographic resolution with cone voltages of –40 V, –50 V, –60 V, and –120 V. This experiment indicated that the loop injections accurately reflected the ionization behavior in all solvent proportions appearing during the gradient analysis and that the regioisomers showed identical ionization behavior (data not shown).

To maximize analytical sensitivity using multi-reaction monitoring, the collision cell voltages must be optimized to produce the highest abundance transition ion, i.e. a characteristic ion from the collision induced dissociation of the molecular ion selected in the first quadrupole. To identify these energies, analytes were separated using a rapid HPLC gradient (0 min = 60% Solvent A, 15 min = 100% Solvent B, flow rate = 350 µl/min) eluting all analytes within 8 min. Product ion spectra were collected for each molecular ion using collision voltages of –8 V, –10 V, –13 V, –17 V, –20 V, –23 V, –26 V, and –30 V.

Method performance and quality control

The presence of target analytes in available urine samples required the use of a non-urine matrix for spike enrichment analyses. Therefore, 4 ml of 0.1 M sodium phosphate (pH 7.4) was used for these analyses and extracted as described below. The analytical accuracy and precision was initially evaluated by analyzing replicate samples (n = 3) enriched with the target analytes at four concentrations ranging from ~0.1–100 nM without β-glucuronidase treatment. Analyses were then repeated at the 1.0 and 10 nM level with β-glucuronidase to evaluate the effect of the incubation on analyte recovery. A blank and a 10 nM level matrix spike were analyzed with each batch of 20 samples to concurrently evaluate methodological performance. The method accuracy was considered acceptable if recovered values were between 75% and 120% of the true value. The method detection limit (MDL) was calculated as three times the standard deviation in triplicate analyses of the lowest spike concentration passing the recovery criterion. The limit of quantification (LOQ) was established at 3× the MDL. Analytical precision was evaluated when analyte concentrations were >LOQ. Precision was considered acceptable if the relative standard deviation in replicate analyses were ≤15%.

To evaluate the influence of the matrix on quantitative results, a standards addition analysis was performed on four urine samples. The samples consisted of a human sample from one

male and one female, one SHR, and one SD rat. Twenty-microliter extract aliquots were enriched with each analytical target at 3, 10, 100, and 1,000 fmol/ μ l, adjusted for a common 5-fold dilution with methanol, and reanalyzed. The regression slopes and quantitative results were compared.

Surrogate recoveries were calculated by independent analysis of these residues relative to the internal standard 20-HE. A three-point calibration was prepared at the time of sample preparation from the surrogate spike solution used for the analysis of samples. These solutions contained 100%, 50%, and 10% equivalent surrogate spikes along with 100% equivalent of the internal standard.

Sample collection and storage

Rodent urine was collected over dry ice in polypropylene tubes containing either 10 mg of triphenylphosphine (TPP) or butylated hydroxytoluene (BHT). The use of TPP to reduce peroxides to their monohydroxy equivalents, or BHT to quench radical catalyzed reactions, both prevent peroxy radical propagated transformations of polyunsaturated fatty acids (39, 40). Human urine was either analyzed immediately or frozen without the addition of TPP or BHT. All samples were stored at $<-20^{\circ}\text{C}$ until analysis.

Rodent urine was collected and analyzed to assess the utility of the procedure in two common rodent models. Twenty-four hour urine samples were collected from SHR ($n = 2$) and SD rats ($n = 2$). Human urine samples were analyzed to establish baseline information. Samples were collected under approved human health protocols by spontaneous evacuation from apparently healthy volunteers. Samples were immediately frozen until analysis. Initial experiments were designed to evaluate the variability in lipid concentrations and profiles. Unless otherwise noted, samples were collected upon the second evacuation of the day. Twenty volunteers participated in this study (nine male and 11 female) with ages ranging from 23–50 years. Collection times ranged from 8:30 AM to 6:10 PM. Within the group, 52% had consumed caffeine: 78% of the men and 36% of the women. Further samples were then collected from a gender-matched subset of this group (three men and three women). These individuals provided a complete series of urine samples from a single day at ~ 3 h intervals (samples ranged from 5–10 per individual). A single individual provided samples for a second day.

Sample analysis

Frozen urine samples were thawed, vortexed and a 50 μ l urine aliquot was diluted 10-fold for creatinine determinations. These dilutions were stored at 4°C for <3 days until analysis. Creatinine concentrations were measured in triplicate using a 96-well plate format kinetic assay; procedure #557 Sigma Diagnostics (St. Louis, MO). Each sample was run against an independent 1–10 mg/dl calibration curve. The resulting values were generally within 5%, but never greater than 10% different. Secondary dilutions were prepared as necessary to bring samples within the calibrated range.

For lipid analyses, 4 ml urine aliquots were transferred to a 15 ml graduated polypropylene tube (Becton Dickson Labware). Human samples, which were not collected with reducing agents or antioxidants, were enriched with ~ 5 mg of BHT. The 4 ml aliquot was then spiked with extraction surrogates: ~ 100 pmol (~ 35 ng) of both 10(11)-EpHep and 10,11-DiHN in 100 μ l of methanol. Preliminary results indicated that lipid diols occurred primarily as glucuronic acid conjugates in human urine. To release dihydroxy lipids from their glucuronides, the spiked samples were incubated for 3 h at 37°C with 400 units of *Helix pomatia* type H-1 β -glucuronidase (Sigma) delivered in 1 ml of 1 M sodium citrate (pH 5.5). Sample pH was confirmed at <6.0 with

pH paper. Negative controls for β -glucuronidase received buffer only. Because β -glucuronidase treatment had no effect on either diol or 20-HETE concentrations in rat urine, subsequent 4 ml rodent urine aliquots were only amended with 1 ml of sodium chloride saturated water prior to extraction. Samples were then vortexed with 2 ml of ethyl acetate and centrifuged. The organic phase was isolated in a 1 dram (~ 4 ml) borosilicate vial (Fisher Scientific) and the extraction was repeated. The combined organic phases were reduced to dryness under nitrogen while held at 50°C . The residue was re-dissolved in 100 μ l of acetonitrile, spiked with 2.5 nmol of 20-HE in 10 μ l of acetonitrile and vortexed. A 50 μ l aliquot was then transferred for analysis. Extracts were stored at -32°C until analysis.

Statistical analysis

Non-parametric statistics were employed for all comparisons due to the limited sample number, and the lack of knowledge of the distribution and variance of the targeted measurements in the experimental population. Correlations were evaluated using the Spearman's rank correlation and the Mann-Whitney U test was employed to differentiate population means. Statistical significance was assigned at the $P < 0.05$ level, unless otherwise noted.

RESULTS

EpOME and DiHOME isomer abundance

A 1:1 mixture of the 9(10)-EpOME and 12(13)-EpOME regioisomers were isolated from the linoleic acid epoxidation reaction. Derivatization followed by GC/MS analysis showed that the sum of the observed isomer masses was within 5% of the weighed mass. After purification, the diol mixture prepared from this epoxide mixture showed a 70:30 isomeric ratio with an excess of 9,10-DiHOME. Shifts in the theoretical 1:1 isomeric abundance have

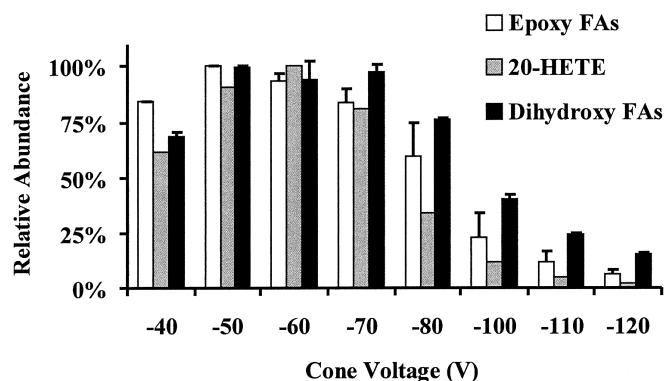


Fig. 1. The effect of cone voltage on pseudo molecular ion intensity. Full scan spectra (m/z 250–350) were collected from 10 μ l loop injection of calibration solutions containing 1 μM of each target analyte and 0.1 μM of each internal standard. Cone voltages were varied from -40 to -120 V as indicated. The total integrated area of the deprotonated molecular ion ($[\text{M}-\text{H}]^-$) from each injection was collected. The normalized mean response \pm SD for the epoxy and dihydroxy compounds shown. Epoxy FAs: epoxyheptadecanoic acid (EpHep), epoxyoctadecenoic acid (EpOME), and epoxyicosatrienoic acid (EET); Dihydroxy FAs: DiHN, dihydroxyoctadecenoic acid (DiHOME), and dihydroxyicosatrienoic acid (DiHET). The only analyzed monohydroxy compound was 20-HETE. Analysis with chromatographic separation confirmed these results and showed equivalent ionization behavior for the analyzed regioisomers.

been previously observed in our laboratory due to the conservative collection of diol regioisomers from the silica gel column.

EET 205 nm molar extinction coefficients

Epoxy fatty acids lack a strong chromophore, limiting the sensitivity of detection based on UV absorption. However, the isomeric extinction coefficients can be used to speciate isomeric mixtures. The molar extinction coefficient (ϵ) is defined as the amount of radiant energy absorbed on a path through a solution of known molar concentration expressed in $\text{Abs mole}^{-1}\text{cm}^{-1}$. This measurement can be performed using HPLC data if the flow cell dimensions, peak width, and flow rate are known. The injected mass divided by the product of the peak width and flow rate will yield the concentration in the detector flow cell producing the aggregate peak area. To calculate the extinction coefficient for each isomer, an injection containing 1.1 nmol of each compound was analyzed in triplicate using the isocratic system and analytical PhaseSep column described above. Absorbance was measured at 205 nm. The flow cell length was 6 mm, the peak width was 0.35

min, and the flow rate was 2 ml/min. The calculated ϵ_{205} for 14(15)-EET ($77,000 \pm 3,500$), 11(12)-EET ($43,300 \pm 1,100$), 8(9)-EET ($41,400 \pm 180$) showed a 1.8:1.1:1.0 ratio. Further analysis of a five-point curve (50–1500 pmol/injection) produced linear curves ($r^2 > 0.998$) with slope ratios matching the ϵ_{205} ratios. The detection limit for 14(15)-EET was ~ 50 pmol. Reanalysis of the original mixture revealed a 3.2:1.4:1.0 ratio of 14(15)-, 11(12)-, and 8(9)-EETs. Therefore, the initial 70 mg aliquot contained ~ 30 , 22.5, and 17.5 mg of each isomer, respectively.

Optimization of MS and MS/MS Parameters

Cone voltage manipulations had a dramatic effect on the intensity of the deprotonated molecular ion ($[\text{M-H}]^-$), as shown in **Fig. 1**. Epoxides showed maximal ionization with a cone voltage of -50V, with $\sim 10\%$ decline at -60V. The ionization of 20-HETE was optimal at -60V and the diols, exhibited nearly equivalent ion intensities between -50 and -70V. Increasing voltages to -120V decreased ion intensity by as much as 90%.

In the Quattro Ultima, the quadrupoles are linked by an octapole collision cell. The voltage applied to the colli-

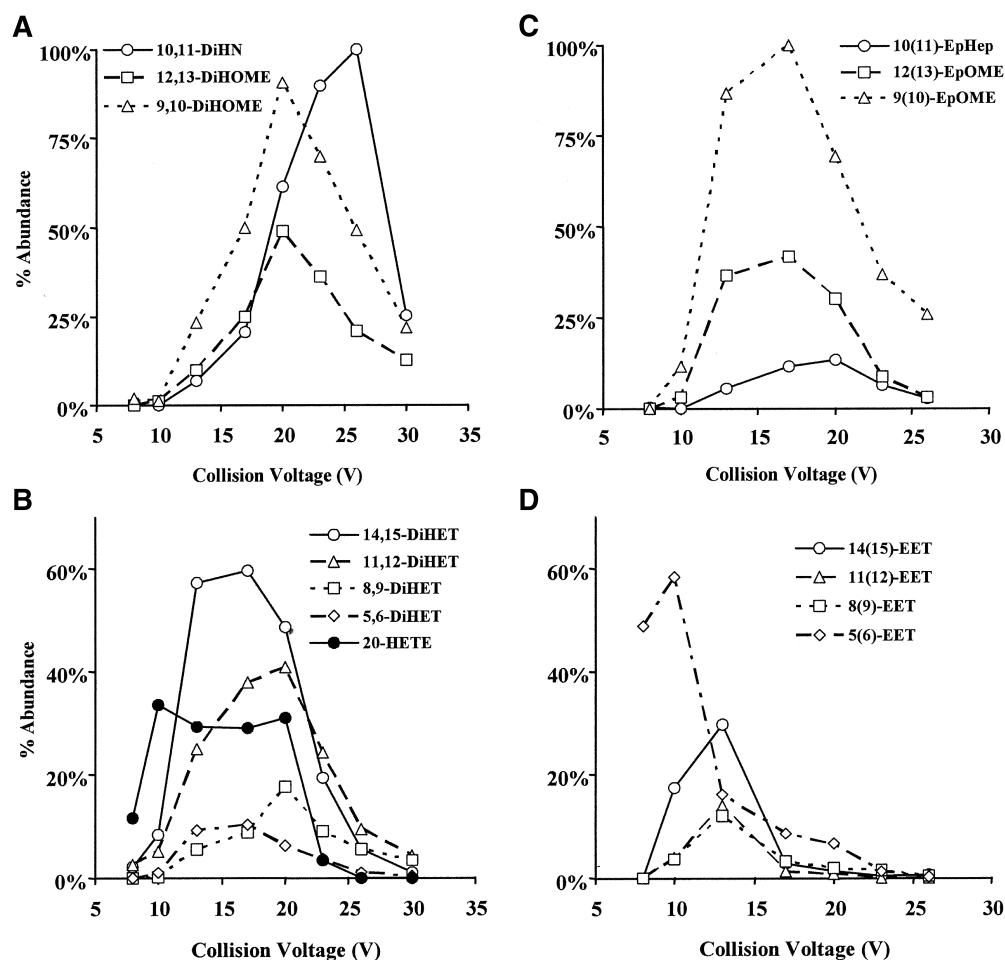


Fig. 2. The collision voltage was optimized to maximize the intensity of selected unique transition ions for each target analyte. A and B: Show dihydroxy fatty acid behavior. C and D: Show epoxides. Ion abundances are normalized to the highest intensity ion produced within each class. (i.e., Diols: 10,11-DiHN, 329 > 311 at 26V; Epoxides: 9(10)-EpOME, 295 > 171 at 17 V).

TABLE 3. Analyte retention times and calibration statistics

Analyte	tR ^{a,b}	Low Calibration Curve ^c	r ²	Full Calibration Curve ^d	r ²
12,13-DiHOME ^e	5.64	y = 1.32x + 4.3	0.9998	y = 1.42x + 8.6	0.9998
9,10-DiHOME ^e	6.12	y = 2.27x + 9.66	1.000	y = 2.14x + 19.6	0.9995
14,15-DiHET ^e	6.66	y = 2.41x + 1.73	0.9998		
11,12-DiHET ^e	7.56	y = 1.95x + 0.541	1.000		
8,9-DiHET ^e	8.34	y = 0.710x - 0.148	0.9999		
5,6-DiHET ^e	9.48	y = 0.776x - 0.343	0.9999		
20-HETE ^f	9.30	y = 0.738x + 1.69	0.9999		
12(13)-EpOME ^f	16.43	y = 0.813x + 11.6	0.9988	y = 0.873x - 29.4	0.9999
14(15)-EET ^f	16.82	y = 0.489x + 0.023	0.9999	y = 0.503x - 5.74	1.000
9(10)-EpOME ^f	17.05	y = 2.08x + 21.9	0.9994	y = 2.06x + 43.8	1.000
11(12)-EET ^f	18.58	y = 0.244x - 0.455	0.9997	y = 0.261x - 6.19	0.9999
8(9)-EET ^f	18.86	y = 0.320x - 1.58	0.9996	y = 0.3310x - 9.00	0.9997
5(6)-EET ^f	19.71	y = 1.27x + 2.20	1.000	y = 1.29x - 4.25	0.9997

^a tR, retention time in minutes.

^b Surrogate tR, 11.4 and 16.49 min for 10,11-DiHN and 10(11)-EpHep, respectively.

^c Calibration from 3 nM–1 μM.

^d C18:1 lipid calibration curve from 3 nM–25 μM, C20:3 lipid calibration curve from 3 nM–10 μM.

^e Calibration curves relative to 1.42 μM 10,11-DiHN.

^f Calibration curves relative to 1.13 μM 10(11)-EpHep.

sion cell leads to the acceleration of the pseudo molecular ion isolated in the first quadrupole into the collision cell gas, leading to collision induced dissociation of the ion. The composition and intensity of the ions produced during this process are a function of the inherent molecular stability and the energies applied. Table 1 and Table 2 display the optimized collision voltage, characteristic transition ions, and positions of molecular fragmentation for each target analyte. The voltage dependence of the selected quantification ion is shown in Fig. 2.

Optimized HPLC conditions and calibration results

The HPLC gradient was optimized for maximum isomeric resolution in minimum analysis time (shot to shot time ~35 min). While analysis times of <10 min were obtainable with these solvent systems, resolution of the DiHOME isomers was required since these tightly eluting isomeric pairs produced common ions upon collision (Table 2). In addition, short run times compromised diol

analysis in urine extracts due to unknown components that produced some of the targeted mass transitions. The optimized HPLC program used a constant flow rate of 350 μl/min and a solvent gradient as follows: 0 min = 100% Solution A, 18 min = 70% Solution A, 20–23 min = 100% Solution B, 25–28 min = 100% Solution A. Analyte retention times and calibration results are shown in Table 3. Excellent linearity was observed for all analytes over an extended concentration range. Representative chromatograms are shown in association with the rat urine analyses below.

Accuracy and precision

Initial matrix spike experiments were conducted without β-glucuronidase treatment. Triplicate aliquots of phosphate buffer were enriched with four concentrations of analytes between 0.1 and 100 nM. The exact concentrations, accuracy, and precision of these analyses are shown in Table 4. With the exception of 5(6)-EET, all detected analytes met the quality control (QC) criterion of 75% to

TABLE 4. Matrix spike recovery without β-glucuronidase treatment^a

Analyte	~0.1 nM Spike	~1 nM Spike	~10 nM Spike	~100 nM Spike
12,13-DiHOME	0.0620 (47 ± 38%) ^b	0.620 (100 ± 8%)	7.80 (111 ± 2%)	62.4 (107 ± 0.1%)
9,10-DiHOME	0.146 (95 ± 29%)	1.46 (95 ± 5%)	18.2 (111 ± 1%)	146 (106 ± 2%)
14,15-DiHET	0.110 (91 ± 22%)	1.10 (107 ± 10%)	6.88 (82 ± 5%)	110 (109 ± 4%)
11,12-DiHET	0.0940 (96 ± 19%)	0.940 (92 ± 4%)	5.84 (85 ± 5%)	93.5 (109 ± 3%)
8,9-DiHET	0.126 (85 ± 13%)	1.26 (92 ± 4%)	7.88 (77 ± 3%)	126 (105 ± 5%)
5,6-DiHET	0.109 (88 ± 28%)	1.09 (81 ± 6%)	6.81 (83 ± 4%)	109 (111 ± 4%)
20-HETE	ND	1.17 (87 ± 5%)	11.7 (76 ± 2%)	97.8 (95 ± 1%)
12(13)-EpOME	ND	1.3 (111 ± 13%)	13.0 (105 ± 2%)	130 (102 ± 1%)
9(10)-EpOME	ND	1.13 (108 ± 10%)	13.0 (107 ± 2%)	130 (103 ± 1%)
14(15)-EET	ND	0.999 (118 ± 14%)	9.99 (104 ± 3%)	99.9 (108 ± 1%)
11(12)-EET	ND	1.00 (106 ± 9%)	10.0 (107 ± 7%)	100 (113 ± 1%)
8(9)-EET	ND	1.00 (106 ± 17%)	10.0 (107 ± 2%)	100 (117 ± 4%)
5(6)-EET	ND	1.17 (13 ± 5%) ^b	11.7 (15 ± 1%) ^b	97.8 (25 ± 4%) ^b

^a Each matrix spike analysis was performed in triplicate. The nM spike concentration is shown with the percent recovery (mean ± SD). All samples passed the precision criterion of <15% variance at concentration > limit of quantification (LOQ). ND, Not detected.

^b Residue exceeds the quality control criterion of 75–120% recovery.

TABLE 5. Matrix spike results with β -glucuronidase treatment^a

Analyte	Spike	Recovery
	<i>nM</i>	%
12,13-DiHOME	3.90	108 ± 2
9,10-DiHOME	9.10	106 ± 3
14,15-DiHET	6.88	101 ± 7
11,12-DiHET	5.84	100 ± 6
8,9-DiHET	7.88	94 ± 4
5,6-DiHET	6.81	273 ± 32 ^b
20-HETE	11.7	84 ± 14
12(13)-EpOME	13.0	102 ± 5
9(10)-EpOME	13.0	103 ± 5
14(15)-EET	10.0	109 ± 8
11(12)-EET	10.0	112 ± 4
8(9)-EET	10.0	117 ± 4
5(6)-EET	11.7	2 ± 1 ^b
5(6)-EET + 5,6-DiHET	18.6	101 ± 11

^a Each matrix spike analysis was performed in triplicate. The nM spike concentration is shown with the percent recovery (mean ± SD). All samples passed the precision criterion of <15% variance at concentration > LOQ. Spikes at the ~1 nM level produced equivalent results (data not shown).

^b Residue exceeds the quality control criterion of 75–120% recovery.

120% recovery. The loss of 5(6)-EET did not result in elevated 5(6)-diol concentrations under these conditions. The corresponding delta lactone may have been formed. Analytical precision was generally excellent. Only the dihydroxy lipids were detected at the 0.1nM level, where replicate precision ranged from 13–38%.

To evaluate the effect of the β -glucuronidase treatment, triplicate buffer samples were then enriched at the ~10 nM level and analyzed as described (Table 5). With the exception of 5,6-DiHET, these results were in good agreement with the analysis performed without β -glucuronidase. Additional analyses were performed at the ~1 nM level with equivalent results (data not shown). In the acidified deconjugation reaction, the sum of the 5(6)-EET and 5,6-DiHET showed recoveries of ~100%. These results suggest that the 5(6)-EET was hydrolyzed to the diol under these conditions.

A detection limit defines the concentration at which a detected residue can be statistically discriminated from noise. The instrumental detection limit (IDL) is the concentration producing a 3:1 signal to noise ratio (S:N) and describes the inherent sensitivity of the instrument. Analysis of calibration standards established the IDL at between 0.5 and 15 fmol/ μ l. This concentration is equivalent to a 0.02 pM to 0.40 pM concentration in a 4 ml urine sample analyzed at a final volume of 100 μ l (Table 6). The method detection limit incorporates all phases of sample extraction and analytical manipulation. This value was calculated as three times the replicate precision of the lowest matrix spike data passing the recovery criterion (Table 4). The calculated MDLs were between 0.01 and 0.5 nM (Table 6). The limit of quantification is statistically defined as the concentration at which the measured value meets the accuracy criterion and has an inherent variance of less than <10% (41). This corresponds to nine times the standard deviation of the low level analysis. Again using the matrix spike data, the LOQ was estimated at between 0.15 nM and 1.5 nM (Table 6). While analytically valid, each of

TABLE 6. Estimated nM detection and quantification limits^a

Compound	IDL ^b	MDL ^c	LOQ ^d	Compound	IDL ^b	MDL ^c	LOQ ^d
12,13-DiHOME	0.06	0.15	0.45	12,13-EpOME	0.1	0.50	1.5
9,10-DiHOME	0.03	0.13	0.39	9,10-EpOME	0.03	0.34	1.0
14,15-DiHET	0.02	0.071	0.22	14(15)-EET	0.1	0.42	1.3
11,12-DiHET	0.02	0.050	0.16	11(12)-EET	0.1	0.27	0.80
8,9-DiHET	0.03	0.050	0.15	8(9)-EET	0.4	0.50	1.5
5,6-DiHET	0.03	0.090	0.27	5(6)-EET	0.01	NA ^e	NA ^e
20-HETE	0.06	0.18	0.53				

^a Detected concentrations (fmol/ μ l) were transformed to equivalent sample nM concentrations (sample volume, 4 ml; final volume, 100 μ l; injection volume, 10 μ l).

^b Instrumental detection limit (IDL): the concentration producing a signal to noise ratio (S:N) of 3:1.

^c Method detection limit (MDL): three times the standard deviation in the lowest concentration matrix spike which passed the QA criterion. This estimate incorporates all method error except sample heterogeneity.

^d LOQ, nine times the standard deviation in the lowest concentration matrix spike which passed the QA criterion.

^e NA, not applicable. The MDL and LOQ is only calculated for residues which met the recovery criterion of 75–120%.

these values still fails to incorporate sampling variability and sample homogeneity. The duplicate analysis of five human urine samples produced 35 residues with concentrations ranging from 0.1–850 nM. The aggregate precision of these results was 14 ± 7%. Only three compounds showed replicate differences ≥15%. Together, these results support a procedural LOQ of ~1 nM, with expectable replicate precision of at least 15%.

Surrogate robustness

A key feature of the described procedure is the use of chemical analogs as extraction surrogates. Surrogate recoveries were comparable between both spiked urine and spiked buffer analyses: DiHN 72 ± 12%; EpHep = 50 ± 10% (n = 54). However, if matrix components alter the relative response factors of the surrogate/analyte pair, bias will be introduced into the quantitative results. To determine if this bias occurred in the current analyses, the target analytes were quantified in four urine samples

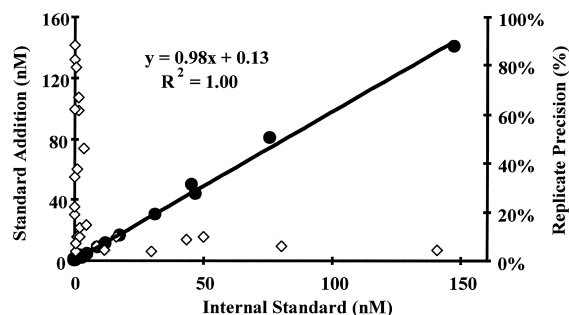


Fig. 3. Internal standard and standard addition methods were used to quantify oxylipids in four urine samples. After the initial analysis, extracts were enriched with four concentrations of analytes (3–1,000 nM). All detected residues and the replicate precision of the two analyses are shown. Closed circles show nM concentrations. Open diamonds show the replicate percent difference. Analytical precision was <15% for all residues detected above 1 nM.

TABLE 7. Ratio of calibration slopes in the presence and absence of urine extracts

Analyte	Human Male	Human Female	SH Rat ^a	SD Rat ^b
12,13-DiHOME	1.0	0.89 ^c	0.98	1.0
9,10-DiHOME	1.1	1.1	1.0	1.1
14,15-DiHET	0.95	1.1	1.1	1.1
11,12-DiHET	0.93	0.94	0.92	1.0
8,9-DiHET	0.99	1.1	0.94	1.1
5,6-DiHET	0.96	1.0	0.93	1.0
12(13)-EpOME	1.0	1.0	1.0	0.91
9(10)-EpOME	0.99	1.0	0.87 ^c	0.89 ^c
14(15)-EET	1.0	1.0	1.0	0.96
11(12)-EET	1.0	1.0	1.2 ^c	0.93
8(9)-EET	1.0	0.93	1.1	0.91

^a Spontaneously hypertensive rat (SHR) (male).

^b Sprague-Dawley rat (SD) (male).

^c Residues showing >10% difference in regression slopes in the presence and absence of matrix.

using both internal standard and standard addition approaches. Enriching extracts with known amounts of each analyte, while maintaining an equivalent surrogate concentration in each sample, allowed for the generation of calibration curves in the presence of each sample extract. The intercept of this regression with the x axis provided the concentration of the target analytes. The calculated data were in good agreement using either technique **Fig. 3**. Since each sample did not contain all of the target analytes, a comparison of the regression slopes in the presence and absence of matrix was also performed. In either the pres-

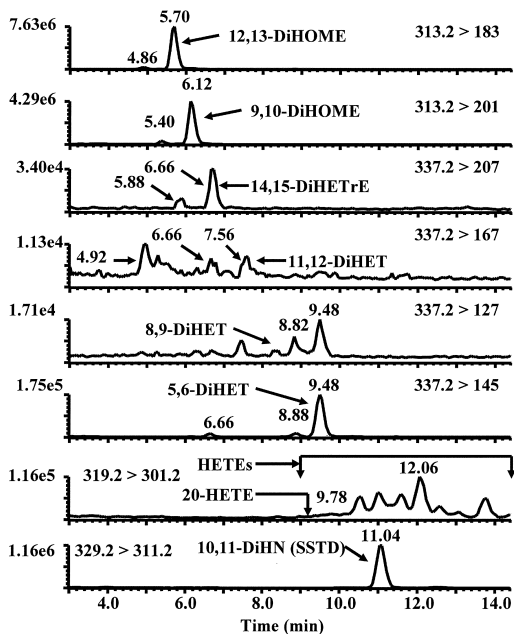


Fig. 4. Using multi-reaction monitoring, numerous dihydroxy and hydroxy fatty acids could be simultaneously detected. This representative series of extracted ion chromatograms show the measured hydroxy fatty acids in the urine of a single spontaneously hypertensive rat. The detected DiHOMEs, DiHETs, HETEs, and the diol extraction surrogate standard (SSTD) DiHN are indicated with arrows. The y axis labels indicate the intensity of the dominant ion within each trace. 20-HETE was not detected.

ence or absence of matrix, the slopes of the calibration curves were within 10% for 40 of 43 (i.e., 93%) of the generated data points (**Table 7**). No single analyte showed a slope deviation of greater than 10% in more than one analysis.

Comparison of urinary oxylipids in two rat strains

Rats provide common experimental models in biological investigations. Glucuronidase treatment caused no change in measured urinary oxylipids from either rat strain (data not shown). Representative extracted ion chromatograms for each analyte and internal standard in rat urine are shown in **Figs. 4** and **5**.

Comparing the 13-week-old SHR and the SD rat urine oxylipids showed a number of key differences, as well as certain similarities. The high variability and low sample number precluded the statistical discrimination of these two rat strains based on concentrations of components in their urine. However, comparing the ratio of each epoxide to its corresponding diol isomer suggested the elevation of epoxides in the SHR strain (**Fig. 6**). In contrast to these differences, both strains showed detectable levels of all target analytes, with the notable exception of 20-HETE. The octadecanoids were present at 10–80 ng/ml, while the eicosanoids were observed at concentrations <1.5 ng/ml. In addition, the relative abundance of regioisomers within each analyte subclass appeared similar

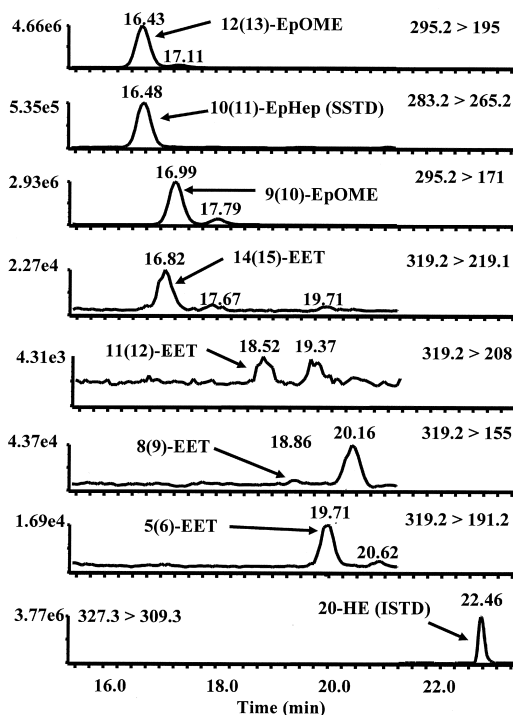


Fig. 5. Using multi-reaction monitoring, numerous epoxy fatty acids could be simultaneously detected. This representative series of extracted ion chromatograms show the measured epoxy fatty acids in the urine of a single spontaneously hypertensive rat. The detected EpOMEs, EETs, the epoxide extraction SSTD, and the internal standard (ISTD) are indicated with arrows. The y -axis labels indicate the intensity of the dominant ion within each trace.

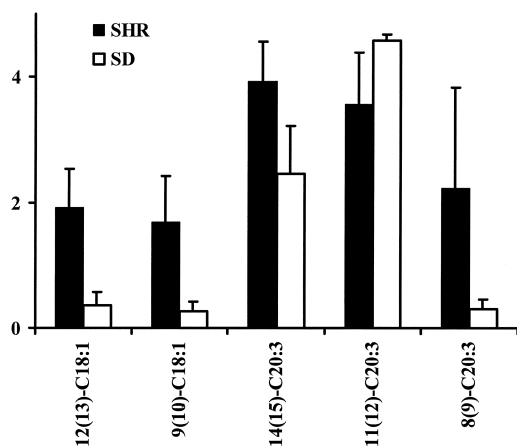


Fig. 6. The epoxide to diol ratios in the urine of 13-week-old spontaneously hypertensive rats (SHR; $n = 2$) and Sprague-Dawley rats (SD; $n = 2$) showed distinct differences. The linoleate and arachidonate derived isomers are denoted as C18:1 and C20:3, respectively. Numbers indicate the position of epoxide and diol moieties. The displayed data are the mean \pm the difference in the two observations.

(Table 8). Specifically, both the EpOME and DiHOME profiles showed $\sim 70:30$ ratios of the 12,13-:9,10-isomers. The DiHETs showed a 40:8:3:2 ratio of 5,6-:14,15-:8,9-:11,12-isomer ratio, while the EETs showed $\sim 8:1:1$ ratios of the 14,15-:11,12-:8,9-epoxides in both strains.

Human urinary oxylipids

Analysis of human urines ($n = 2$, one male one female) with and without β -glucuronidase indicated that $<1\%$ of the detected diol residues were present in the urine unconjugated. Therefore, all human urine samples were analyzed with β -glucuronidase treatment. The inter-individual variability in the second urine evacuation of the day was high (Table 9). No discernable differences were observed between males and females or in the presence or absence of caffeine in the diet. No correlation was observed between subject age and urinary lipid levels. A weak correlation was observed between analyte concentra-

TABLE 9. Human urinary oxylipids in pmol/mg creatinine ($n = 20$)

Analyte	n^a	Range	Geometric Mean
12,13-DiHOME	20	1.05 – 58.5	9.58
9,10-DiHOME	20	9.90 – 497	97.5
14,15-DiHET	20	0.0682 – 1.85	0.562
11,12-DiHET	20	0.0222 – 0.590	0.198
8,9-DiHET	20	0.357 – 11.0	1.98
5,6-DiHET	20	0.0625 – 1.03	0.321
20-HETE	19	0.00451 – 2.63	0.230 ^b
12(13)-EpOME	14	0 – 0.798	0.082 ^b
9(10)-EpOME	3	0 – 0.281	0.025 ^b
14(15)-EET	17	0 – 0.239	0.069 ^b
11(12)-EET	4	0 – 0.0936	0.013 ^b
8(9)-EET	5	0 – 1.134	0.047 ^b

^a Number of subjects with concentrations of the indicated analyte greater than the MDL.

^b Non-detected residues were replaced with 0.005 for calculation of geometric means. Creatinine values ranged from 26–389 mg/dl; geometric mean = 109 mg/dl.

tions and the time of the second evacuation ($P = \sim 0.2$). To further clarify this analysis, the sample set was segregated by collection time into three groups: I = before 10 AM ($n = 9$), II = between 10 AM and 1 PM ($n = 7$), III = after 1 PM ($n = 4$). Comparison of these groups supported the weak correlation and showed statistically higher concentrations of 9,10-DiHOME, 12,13-DiHOME, and 8,9-DiHET in second evacuations occurring late in the day (Fig. 7). Regardless of concentration or gender, lipid subclass composition was generally consistent among groups (Table 10). However, the relative abundance of 8(9)-EET appeared to decrease from the morning to the evening. In all cases, 9,10-DiHOME was $\sim 90\%$ of the DiHOME profile, while 8,9-DiHET was $\sim 70\%$ of the DiHET profile.

Diurnal variation in human urine

The time dependent differences in urinary concentrations suggested that the duration of urine accumulation and/or the time of collection influenced the concentrations observed in the final analysis. To evaluate the potential for diurnal variations of oxylipid elimination in the

TABLE 8. Composition of oxylipid subclasses in the urine of two rat strains^a

Strain	$\frac{12(13) - EpOME}{9(10) - EpOME}$	$\frac{12,13 - DHOME}{9,10 - DHOME}$	$\frac{14,15 - EpETrE}{11,12 - EpETrE}$ $\frac{8,9 - EpETrE}{8,9 - EpETrE}$	$\frac{14,15 - DHETrE}{11,12 - DHETrE}$ $\frac{8,9 - DHETrE}{5,6 - DHETrE}$
	SHR ^b	$70 \pm 1\%$ $30 \pm 1\%$	$67 \pm 3\%$ $32 \pm 3\%$	$81 \pm 7\%$ $7 \pm 1\%$ $12 \pm 7\%$
SD ^c	$73 \pm 2\%$ $27 \pm 2\%$	$65 \pm 4\%$ $35 \pm 4\%$	$79 \pm 12\%$ $13 \pm 9\%$ $8 \pm 4\%$	$16 \pm 4\%$ $1 \pm 1\%$ $4 \pm 6\%$ $78 \pm 1\%$

^a Displayed data represents the mean \pm the relative percent difference between the two observations.

^b SHR, 13-week-old spontaneously hypertensive rat ($n = 2$).

^c SD, Sprague-Dawley rat ($n = 2$).

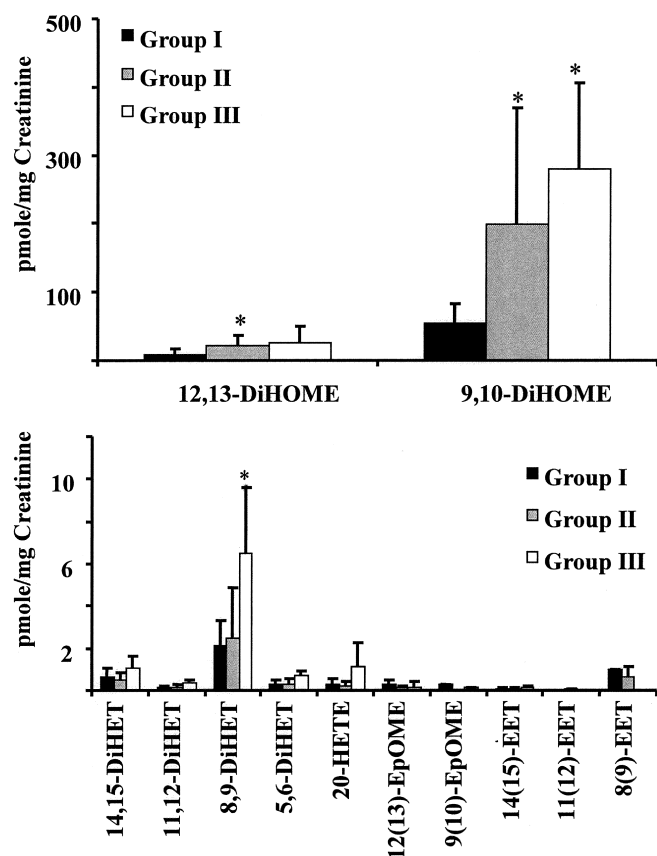


Fig. 7. Urine collected later in the day showed higher dihydroxy fatty acid concentrations in human subjects. Collected urine samples represent the second daily spontaneous evacuation. Subjects were segregated into three groups by collection time: before 10 AM (Group I; n = 9), between 10 AM and 1 PM (Group II; n = 7) or after 1 PM (Group III; n = 4). The mean \pm SD of each data set is shown. Statistical elevations in the DiHOMEs and 8,9-DiHET were observed in mid-day and late collections, relative to morning collections (* $P < 0.05$).

urine of humans, sequential samples were collected from six individuals (three male, three female) at approximately 3 h intervals. Creatinine concentrations showed fluctuations over the course of the day (3–4-fold in females: F1 = 51 – 194 mg/dl, F2 = 58 – 173 mg/dl, F3 = 159 – 480 mg/dl; 2–12-fold in males: M1 = 12 – 156 mg/dl, M2 = 154 – 311 mg/dl, M3 = 22 – 259 mg/dl). Four of the six individuals (F1, F3, M1, and M3) showed higher creatinine concentrations in the morning and evening, while the other two individuals showed relatively constant levels. No clear trend was observed for epoxy and monohydroxy fatty acids, which were detected at concentrations below the LOQ (<0.1 pmol/mg creatinine). The diols fluctuated over the course of the day. In both men and women, the DiHOMEs were elevated in the morning and declined in concentrations until 12 AM (Fig. 8). Maximum fluctuations were ~25 fold. The urinary concentration of 9,10-DiHOME returned to morning levels in the women between 3 PM and 6 PM, and surpassed initial concentration in all subjects in the final collection of the day. In contrast, the urinary concentrations in the men remained relatively low in two of three subjects. In contrast to the gender specific stability of DiHOME profiles, the DiHETs showed greater variability in excretion patterns. As indicated earlier, 8,9-DiHET was the dominant isomer at all times in urine samples. In two of three women (ages 26- and 28-years-old), the concentration of 8,9-DiHET increased to a maximum at 3 PM and declined to a minimum between 9 PM and midnight (Fig. 9). In the final female subject (aged 49 years), the concentration of 8,9-DiHET showed maximums in the morning and evening, as observed for the 9,10-DiHOME. The maximum fluctuation in 8,9-DiHET was ~4-fold. The three male subjects also showed significant variability with one showing no changes during the day followed by a 5-fold increase from 9 PM to 1:30 AM. The other two male subjects showed either no detectable

TABLE 10. Composition of oxylipid subclasses in human urine^a

Collection Group	$\frac{12(13) - EpOME}{9(10) - EpOME}$	$\frac{12,13 - DHOME}{9,10 - DHOME}$	$\frac{14(15) - EpETrE}{11(12) - EpETrE}$ $\frac{8(9) - EpETrE}{8(9) - EpETrE}$	$\frac{14,15 - DHETrE}{11,12 - DHETrE}$ $\frac{8,9 - DHETrE}{5,6 - DHETrE}$
Group I	$\frac{4 \pm 11\%}{96 \pm 11\%}$	$\frac{15 \pm 9\%}{85 \pm 9\%}$	$\frac{12\%}{0\%}$ 88%	$\frac{20 \pm 6\%}{5 \pm 2\%}$ $\frac{66 \pm 7\%}{9 \pm 2\%}$
Group II	$\frac{0\%}{100\%}$	$\frac{12 \pm 8\%}{88 \pm 8\%}$	$\frac{25 \pm 32\%}{8 \pm 13\%}$ 67 \pm 45%	$\frac{17 \pm 6\%}{5 \pm 2\%}$ $\frac{67 \pm 9\%}{10 \pm 4\%}$
Group III	ND	$\frac{8 \pm 5\%}{92 \pm 5\%}$	$\frac{87 \pm 6\%}{13 \pm 6\%}$ 0 \pm 0%	$\frac{12 \pm 1\%}{4 \pm 0\%}$ $\frac{75 \pm 3\%}{9 \pm 2\%}$

^a The second daily evacuation was collected before 10 AM (Group I; n = 9), between 10 AM and 1 PM (Group II; n = 7), or after 1 PM (Group III; n = 4). Results are the calculated mean \pm SD for each group.

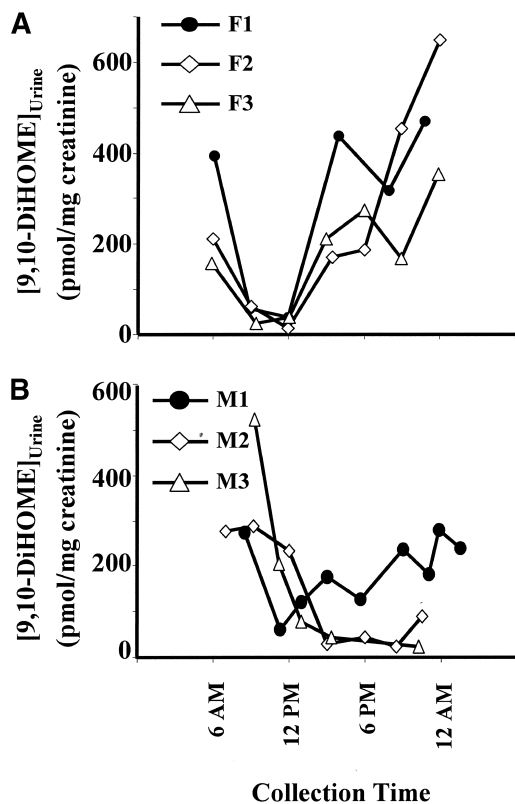


Fig. 8. The concentration of 9,10-DiHOME in human urine showed diurnal variations. Samples were collected on ~ 3 h intervals from three women and three men and analyzed as described. Results were expressed in pmol/mg creatinine. Panels A and B show the female and male subjects, respectively. Subject age: F1, 49 years; F2, 28 years; F3, 26 years; M1, 33 years; M2, 43 years; M3, 35 years.

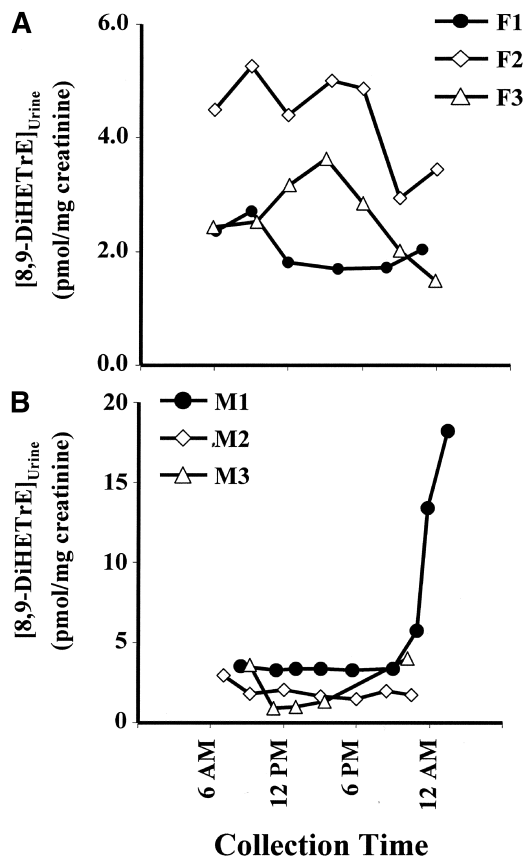


Fig. 9. The concentration of 8,9-DiHET showed diurnal variation in human urine. Samples were collected on ~ 3 h intervals from three women and three men and analyzed as described. Results were expressed in pmol/mg creatinine. A and B: Show the female and male subjects, respectively. Subject age: F1, 49 years; F2, 28 years; F3, 26 years; M1, 33 years; M2, 43 years; M3, 35 years.

change or only a modest fluctuation in the concentrations of this isomer, even though samples were collected as late as 12 AM.

To assess the stability of the observed fluctuations, samples from a single subject (M3) were collected and analyzed for a second day (**Fig. 10**). In this individual a clear cyclical fluctuation of DiHOMEs was observed with a frequency of ~ 24 h and amplitude of ~ 25 -fold. While less definitive, the 14,15-DiHET and 5,6-DiHET appeared to follow this same frequency of oscillation. The 8,9-DiHET and 11,12-DiHET isomer pairs tracked each other and appeared to have a slightly different pattern of change over the course of the day. The magnitude of the DiHET oscillation was ~ 5 -fold. Creatinine normalizations altered the magnitude, but not the pattern of lipid changes observed.

DISCUSSION

The biological significance of the fatty acid epoxygenase pathway is receiving increased attention, primarily driven by activity of the epoxides of arachidonic acid. These agents are endogenous regulators of vascular function, renal ion balance, and inflammation (1). The occur-

rence and function of other polyunsaturated fatty acid epoxides have received less attention. However, elevations in linoleate derived epoxides and/or diols have been identified in several severe medical conditions including generalized peroxisomal disorders (10), rheumatoid arthritis (42), and severe burn cases (43). In turn, the DiHOMEs, or leukotoxin diols, are mitochondrial toxins (29, 30). The described method was developed as a rapid means for the simultaneous quantification of arachidonate and linoleate oxidation products derived from cytochrome P450 metabolism. The analysis focused on the epoxides and diols but also included 20-HETE, which is physiologically linked to vascular regulation.

The presented procedure implements internal standard methodology, solvent extraction, and MS/MS for detection. The use of internal standard methods greatly reduces the systematic error in quantification procedures. By definition, a surrogate standard (SSTD) is an internal standard (ISTD) introduced into the sample prior to extraction. In mass spectrometry, isotopically labeled analogs make the best SSTDs since they retain the chromatographic and ionization behavior of the target with the addition of a discriminatory mass. To the best of our knowl-

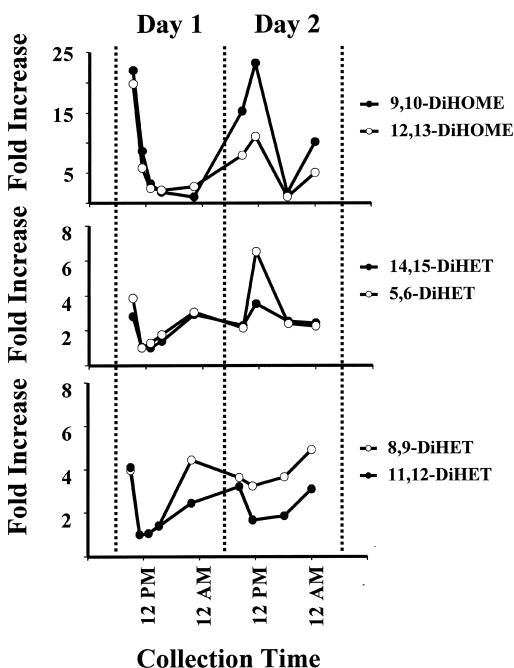


Fig. 10. Analysis of the urine from a 35-year-old male subject over 2 days showed cyclical patterns in dihydroxy lipid concentrations. The fold increase was calculated as the ratio of the value at each collection time and the minimum value over the 2-day collection period. The isomers were segregated by apparent patterns in to three panels.

edge, all published techniques for the LC/MS analysis of oxidized fatty acids have used isotopically labeled analytical surrogates. The primary drawback to the use of labeled surrogates is the cost and analytical complexity when multiple analytical targets are being measured. Here we have investigated the use of odd chain length analogs as SSTDs to reduce the cost and effort to implement this procedure. However, to use chemical analogs as SSTDs, the relative extraction efficiencies must be confirmed. In addition, biases resulting from altered ionization efficiency in the presence of sample matrices must be excluded since these analytes do not chromatographically co-elute with their analytical partner. Matrix spike analyses with or without β -glucuronidase treatment showed that with the exception of the 5(6)-EET, the surrogates performed well in a matrix free environment. These results suggest the procedure will perform well for both cell culture and in vitro metabolism studies, and preliminary evaluations support this conclusion (data not shown). To evaluate the influence of unknown components in urine on surrogate performance, a sample series was analyzed using standard addition methods. If matrix components affected the relative ionization behavior of the SSTD analyte pair, deviations would be expected in both the analytical results and the slopes of the generated regression lines in the presence and absence of matrix. Neither was the case, supporting the applicability of the selected chemical analogs as analytical SSTDs in the developed method.

In addition, it was hoped that the application of tandem

mass spectrometry would allow for shortened analytical run times, relative to those reported for EET analyses. Prior HPLC based procedures have required analytical runs of ~ 40 min for single quadrupole mass spectral detection (44) and >90 min for HPLC using fluorescence detection after derivatization (45). The current procedure is faster than these methods with 5(6)-EET eluting at 20 min, rather than >30 min. Shot to shot run time is 31 min with the described method. The current procedure can be run at a faster pace, however, some analytical accuracy will be sacrificed due to poor isomer resolution. In terms of sensitivity, for the dihydroxy and mono-hydroxy compounds, instrumental detection limits of ~ 10 fmol/injection (3 pg/injection) were achieved, similar to that achieved with other procedures (14, 44–46). For the epoxides, sensitivities of between 40–160 fmol/injection (10–50 pg/injection) were realized, or 10- to 50-fold less sensitive than the selected ion monitoring technique of Nithipatikom et al. (44). Therefore, the use of multi-reaction monitoring sacrifices some sensitivity for the epoxides due to numerous sites of analyte fragmentation.

Regardless of the lower sensitivity of the LC/MS/MS method as compared with other published procedures, the analysis of rat and human urines showed the ability of the method to detect epoxides and diols at physiologically relevant concentrations in urine. Preliminary analyses of human urine showed extremely low epoxide levels. Therefore, to confirm the ability of the method to detect these metabolites in real samples, a minimal number of rodent samples were included from strains previously reported to excrete epoxy fatty acids. Spontaneously hypertensive rats are genetically selected strains that develop age-dependent hypertension (47, 48), which have defects in arachidonic acid epoxygenase and hydroxylase metabolism. Specifically, elevated activity of renal omega hydroxylases (14), epoxygenases, and soluble epoxide hydrolase (49) have been reported. In contrast, the Sprague-Dawley rat is a normotensive strain. The EETs, DiHETs, and 20-HETE have been reported in the urine of these rodents (14, 49).

In this study, 20-HETE was not detected in the urine of either rat strain. Using fluorescence based methods, Maier et al. detected 20-HETE in 10–12-week-old SHR and SD rats at concentrations of ~ 130 and 90 ng/ml (~ 300 nM and 200 nM) assuming 15 ml urine excretion per day (14). These levels are substantially greater than our estimated LOQ. We have no clear explanation for this discrepancy. The animals used by Maier et al. were purchased from Harlan Sprague-Dawley (Indianapolis, IN) rather than Charles River Laboratories and differences between these colonies may be responsible. Since 20-HETE can be transformed into vasoactive ω -hydroxy prostanoids by cyclooxygenase (50), if this activity was elevated in the animals from the current study, urinary 20-HETE concentrations would hypothetically be lowered.

It has been reported that the Charles River Laboratories SHR has elevated renal sEH activity and higher urinary concentrations of DiHETs than the progenitor Wistar-Kyoto rat, a normotensive strain (49). The low sample number in this study precludes statistical comparison of

the hypertensive and normotensive strains, which was not the goal of this study. However, the DiHET concentrations in the SHR urine also appear higher than those in the SD rat. The over expression of sEH in the SHR kidney was expected to reduce urinary epoxide concentrations in the hypertensive strain. However, comparing the epoxide to diol ratios in the urine of the two rat strains showed that in the SHR, epoxide concentrations were elevated with respect to their corresponding diol. Since the epoxides are generally vasodilatory, one would expect the elevated epoxides to correspond to a hypotensive state. These results suggest that the elevated epoxygenase activity (51, 52) in the SHR may be a corrective response to the elevated sEH activity in this rat strain. This possibility remains to be evaluated.


In humans the sum of the detected EETs were close to the method detection limit and ranged from 0.2–2.0 pmol/mg creatinine, or ~0.2–2 nM. Toto et al. reported ~2 nM of total EETs in 24 h urine collections from healthy women (11). Epoxide concentrations in rats were considerably higher. While the method performed equally well for the detection of 20-HETE in matrix spike analyses (LOQ = 0.5 nM), this limit of quantification is 10-fold below levels reported in the urine of children by Watzet et al. (11). The detection of exceedingly low levels of 20-HETE (ND – 2.6 pmol/mg creatinine) in these healthy adults suggest further concentration of extracts prior to analysis maybe beneficial. Currently, 4 ml samples are analyzed at a final volume of 100 μ l. Reducing the final volume or increasing the initial urine volume will be simple means to provide additional sensitivity if necessary.

Comparison of rat and human urine oxylipid profiles showed distinct differences in both isomer abundance and composition. While rats excreted high levels of epoxides, these humans did not (<1 pmol/mg creatinine). In addition, the human subjects primarily excreted hydroxyl fatty acids as glucuronide conjugates while the rats eliminated the parent lipid. Regardless of strain, the rats predominantly formed the 12,13- and 5,6- oxidation products of linoleate and arachidonate, respectively. The human profiles were dominated by the 9,10- and 8,9-isomers of linoleate and arachidonate, respectively. These results suggest either differences in constitutive CYP epoxygenase expression in of these two species, or at least differences in the substrate specificity of the expressed isoforms.

The dominance of the 8,9-oxidation products of arachidonic acid over the 14,15- and 11,12-isomers is in agreement with the previous findings in non-pregnant subjects (13). However, in pregnancy increased urinary levels of 11,12- and 14,15-EETs were reported (13). Catella et al. quantified epoxy fatty acids after chemical hydrolysis with perchloric acid (13). While we have confirmed that this sample acidification does not hydrolyze lipid glucuronides (data not shown), it remains unclear if the measured diols corresponded to epoxides, unconjugated diols, or possibly other acid sensitive conjugates in the urine.

Perhaps of greater importance is the documentation of diurnal cycles in dihydroxy-glucuronide fatty acid elimination in the urine of healthy human subjects. To our knowledge, this is the first such data to be reported. The impli-

cations of these cycles are not known. However, knowing they exist will aid in studies designed to identify associations between these biochemical markers and disease. It is also of particular interest that the DiHOMEs were ~100-fold more concentrated than the DiHETs. In addition, the DiHOMEs fluctuated 25-fold, while the DiHET only changed 5-fold in the urine. Therefore, two orders of magnitude separate the endogenous concentrations of arachidonate and linoleate metabolites derived from the same biochemical cascade. This information should be considered when interpreting the biological relevance of in vitro assays. These data also indicate that the EpOME-DiHOME ratios may be an indication of relative epoxygenases and epoxide hydrolase levels, which can be detected using significantly lower sample volumes.

In conclusion, thorough careful optimization a robust method was produced for the simultaneous quantification of linoleate and arachidonate derived oxidation products using chemical analogs as extraction surrogates. The method shows clear potential for rapid expansion to include additional bioactive oxidized lipids, including other HETE isomers as well as the analogous hydroxy octadecanoids, 9- and 13-hydroxyoctadecadienoic acid. Extension of the procedure for the analysis of serum and tissue samples in experimental animals, as well as serum from humans, will provide insights into the regulatory role of these oxylipids, which may provide useful diagnostic tools in conjunction with the described urine analysis. As is, the method shows that metabolites of linoleate and arachidonate can be determined simultaneously and may provide novel insight into the interaction of these agents in various physiological states. It remains to be seen, however, if urinary profiles reflect a systemic integration of the epoxygenase cascade or simply localized renal activity. 

Funding for this research was provided by National Institute for Environmental Health Sciences Grant R37 ES02710; National Institute for Environmental Health Sciences Superfund Basic Research Program Grant P42 ES04699; National Institute for Environmental Health Sciences Center for Environmental Health Sciences Grant P30 ES05705; and National Institute for Environmental Health Sciences Center for Children's Environmental Health & Disease Prevention Grant 1 P01 ES11269. J.W.N. was supported in part by National Institute for Environmental Health Sciences Training Grant T32 ES07059. The authors would like to thank Dr. Katja Dettmer for many useful discussions and Dr. John Imig at the Medical College of Georgia (Augusta, GA) for the analyzed Sprague-Dawley rat urine.

REFERENCES

1. Capdevila, J. H., J. R. Falck, and R. C. Harris. 2000. Cytochrome P450 and arachidonic acid bioactivation: molecular and functional properties of the arachidonate monooxygenase. *J. Lipid Res.* **41**: 163–181.
2. Roman, R. J. 2001. P-450 metabolites of arachidonic acid in the control of cardiovascular function. *Physiol. Rev.* **82**: 131–185.
3. Zhang, Y., C. L. Oltman, T. Lu, H. C. Lee, K. C. Dellsperger, and M. VanRollins. 2001. EET homologs potently dilate coronary microvessels and activate BK(Ca) channels. *Am. J. Physiol. Heart Circ. Physiol.* **280**: H2430–2440.

4. Draper, A. J., and B. D. Hammock. 2000. Identification of CYP2C9 as a human liver microsomal linoleic acid epoxygenase. *Arch. Biochem. Biophys.* **376**: 199–205.
5. Sevanian, A., J. F. Mead, and R. A. Stein. 1978. Epoxides as products of lipid auto-oxidation in rat lungs. *Lipids.* **14**: 634–643.
6. Iwase, H., T. Takatori, H. Nijima, M. Nagao, T. Amano, K. Iwadate, Y. Matsuda, M. Nakajima, and M. Kobayashi. 1997. Formation of leukotoxin (9,10-epoxy-12-octadecenoic acid) during the autoxidation of phospholipids promoted by hemoproteins. *Biochim. Biophys. Acta.* **1345**: 27–34.
7. Möllenberg, A., and G. Spiteller. 2000. Transformations of 12,13-epoxy-11-hydroxy-9-octadecanoic acid and 4,5-N-acetyl sphingosine by incubation with liver homogenate and liver microsomes. *Z. Naturforsch.* **55c**: 981–986.
8. Greene, J. F., J. W. Newman, K. C. Williamson, and B. D. Hammock. 2000. Toxicity of epoxy fatty acids and related compounds to cells expressing human soluble epoxide hydrolase. *Chem. Res. Toxicol.* **13**: 217–226.
9. Weintraub, N. L., X. Fang, T. L. Kaduce, M. VanRollins, P. Chatterjee, and A. A. Spector. 1999. Epoxide hydrolases regulate epoxyeicosatrienoic acid incorporation into coronary endothelial phospholipids. *Am. J. Physiol.* **277**: H2098–2108.
10. Street, J. M., J. E. Evens, and M. R. Natowicz. 1996. Glucuronic acid-conjugated dihydroxy fatty acids in the urine of patients with generalized peroxisomal disorders. *J. Biol. Chem.* **271**: 3507–3516.
11. Watzer, B., S. Reinalter, H. W. Seyberth, and H. Schweer. 2000. Determination of free and glucuronide conjugated 20-hydroxyarachidonic acid (20-HETE) in urine by gas chromatography/negative ion chemical ionization mass spectrometry. *Prostaglandins Leukot. Essent. Fatty Acids.* **62**: 175–181.
12. Toto, R., A. Siddhanta, S. Manna, B. Pramanik, J. R. Falck, and J. Capdevila. 1987. Arachidonic acid epoxygenase: Detection of epoxyeicosatrienoic acids in human urine. *Biochim. Biophys. Acta.* **919**: 132–139.
13. Catella, F., J. A. Lawson, D. J. Fitzgerald, and G. A. FitzGerald. 1990. Endogenous biosynthesis of arachidonic acid epoxides in humans: increased formation in pregnancy-induced hypertension. *Proc. Natl. Acad. Sci. USA.* **87**: 5893–5897.
14. Maier, K. G., L. Henderson, J. Narayanan, M. Alonso-Galicia, J. R. Falck, and R. J. Roman. 2000. Fluorescent HPLC assay for 20-HETE and other P-450 metabolites of arachidonic acid. *Am. J. Physiol. Heart Circ. Physiol.* **279**: H863–871.
15. Tsikas, D. 1998. Application of gas chromatography-mass spectrometry and gas chromatography-tandem mass spectrometry to assess in vivo synthesis of prostaglandins, thromboxane, leukotrienes, isoprostanes and related compounds in humans. *J. Chromatogr. B. Biomed. Appl.* **71**: 201–245.
16. Schwedhelm, E., D. Tsikas, T. Durand, F-M. Gutzki, A. Guy, J-C. Rossi, and J. C. Froelich. 2000. Tandem mass spectrometric quantification of 8-iso-prostaglandin F2alpha and its metabolite 2,3-dinor-5,6-dihydro-8-iso-prostaglandin F2alpha in human urine. *J. Chromatogr. B. Biomed. Appl.* **744**: 99–112.
17. Tsikas, D., F-M. Gutzki, M. Boehme, I. Fuchs, and J. C. Froelich. 2000. Solid- and liquid-phase extraction for the gas chromatographic-tandem mass spectrometric quantification of 2,3-dinor-thromboxane B2 and 2,3-dinor-6-oxo-prostaglandin F1alpha in human urine. *J. Chromatogr. A.* **885**: 351–359.
18. Rahman, M., J. T. Wright, and J. G. Douglas. 1997. The role of the cytochrome p450-dependent metabolites of arachidonic acid in blood pressure regulation and renal function: A review. *Am. J. Hypertens.* **10**: 356–365.
19. Zou, A. P., J. T. Fleming, J. R. Falck, E. R. Jacobs, D. Gebremedhin, D. R. Harder, and R. J. Roman. 1996. 20-HETE is an endogenous inhibitor of the large-conductance Ca(2+)-activated K+ channel in renal arterioles. *Am. J. Physiol.* **270**: R228–237.
20. Campbell, W. B., D. Gebremedhin, P. F. Pratt, and D. R. Harder. 1996. Identification of epoxyeicosatrienoic acids as endothelium-derived hyperpolarizing factors. *Circ. Res.* **78**: 415–423.
21. Dumoulin, M., D. Salvail, S. B. Gaudreault, A. Cadieux, and E. Rousseau. 1998. Epoxyeicosatrienoic acids relax airway smooth muscles and directly activate reconstituted KCa channels. *Am. J. Physiol.* **275**: L423–431.
22. Fisslthaler, B., R. Popp, U. R. Michaelis, L. Kiss, I. Fleming, and R. Busse. 2001. Cyclic stretch enhances the expression and activity of coronary endothelium-derived hyperpolarizing factor synthase. *Hypertension.* **38**: 1427–1432.
23. Chacos, N., J. Capdevila, J. R. Falck, C. Martin-Wixtrom, S. S. Gill, B. D. Hammock, and R. A. Estabrook. 1983. The reaction of arachidonic acid epoxides (epoxyeicosatrienoic acids) with cytosolic epoxide hydrolase. *Arch. Biochem. Biophys.* **233**: 639–648.
24. Oltman, C. L., N. L. Weintraub, M. VanRollins, and K. C. Dell-sperger. 1998. Epoxyeicosatrienoic acids and dihydroxyeicosatrienoic acids are potent vasodilators in the canine coronary micro-circulation. *Circ. Res.* **83**: 932–939.
25. VanRollins, M., T. L. Kaduce, H. R. Knapp, and A. A. Spector. 1993. 14,15-Epoxyeicosatrienoic acid metabolism in endothelial cells. *J. Lipid Res.* **34**: 1931–1942.
26. Jude, A. R., J. M. Little, J. P. Freeman, J. E. Evans, A. Radominska-Pandya, and D. F. Grant. 2000. Linoleic acid diols are novel substrates for human UDP-glucuronosyltransferases. *Arch. Biochem. Biophys.* **380**: 294–302.
27. Sacerdoti, D., M. Balazy, P. Angeli, A. Gatta, and J. C. McGiff. 1997. Eicosanoid excretion in hepatic cirrhosis. Predominance of 20-HETE. *J. Clin. Invest.* **100**: 1264–1270.
28. Wang, M. H., B. A. Zand, A. Nasjletti, and M. Laniado-Schwartzman. 2002. Renal 20-hydroxyeicosatetraenoic acid synthesis during pregnancy. *Am. J. Physiol. Regul. Integr. Comp. Physiol.* **282**: R383–389.
29. Moran, J. H., T. Mon, T. L. Hendrickson, L. A. Mitchell, and D. F. Grant. 2001. Defining mechanisms of toxicity for linoleic acid monoepoxides and diols in Sf-21 cells. *Chem. Res. Toxicol.* **14**: 431–437.
30. Sisemore, M. F., J. Zheng, J. C. Yang, D. A. Thompson, C. G. Plopper, G. A. Cortopassi, and B. D. Hammock. 2001. Cellular characterization of leukotoxin diol-induced mitochondrial dysfunction. *Arch. Biochem. Biophys.* **392**: 32–37.
31. Slim, R., B. D. Hammock, M. Toborek, L. W. Robertson, J. W. Newman, C. H. Morisseau, B. A. Watkins, V. Saraswathi, and B. Hennig. 2001. The role of methyl-linoleic acid epoxide and diol metabolites in the amplified toxicity of linoleic acid and polychlorinated biphenyls to vascular endothelial cells. *Toxicol. Appl. Pharmacol.* **171**: 184–193.
32. Smith, D. L., and A. L. Willis. 1987. A suggested shorthand nomenclature for the eicosanoids. *Lipids.* **22**: 983–986.
33. Smith, W. L., P. Gorgeat, M. Hamberg, L. J. Roberts II, A. L. Willis, S. Yamamoto, P. W. Ramwell, J. Rokach, B. Samuelsson, E. J. Corey, and C. R. Pace-Asciak. 1990. Nomenclature. In *Methods in Enzymology*. F. A. Fitzpatrick, editor. Academic Press, Inc., San Diego, CA. 1–9.
34. Kiss, L., H. Schutte, K. Mayer, H. Grimm, W. Padberg, W. Seeger, and F. Grimminger. 2000. Synthesis of arachidonic acid-derived lipoxigenase and cytochrome P450 products in the intact human lung vasculature. *Am. J. Respir. Crit. Care Med.* **161**: 1917–1923.
35. Gunstone, F. D., and H. R. Schuler. 1975. Fatty acids, part 45. Epoxyoctadecenoates, dihydroxyoctadecenoates, and diepoxyoctadecanoates: preparation, chromatographic properties, and reactions with boron trifluoride etherate. *Chem. Phys. Lipids.* **15**: 174–188.
36. Murray, R. W., and M. Singh. 1997. Synthesis of epoxides using dimethyl-dioxirane: trans-stilbene oxide. In *Organic Synthesis*. I. Shinkai, editor. John Wiley & Sons, New York. 91–100.
37. Newman, J. W., and B. D. Hammock. 2001. Optimized thiol derivatizing reagent for the mass spectral analysis of disubstituted epoxy fatty acids. *J. Chromatogr. A.* **925**: 223–240.
38. Falck, J. R., P. Yadagiri, and J. Capdevila. 1990. Synthesis of Epoxyeicosatrienoic Acids and Heteroatom Analogs. In *Methods in Enzymology: Arachidonate related lipid mediators*. F. A. Fitzpatrick, editor. Academic Press, Inc., San Diego, CA. 357–364.
39. Nourooz-Zadeh, J., J. Tajaddini-Sarmadi, and S. P. Wolff. 1994. Measurement of plasma hydroperoxide concentrations by the ferrous oxidation-xylenol orange assay in conjunction with triphenylphosphine. *Anal. Biochem.* **220**: 403–409.
40. Carlin, G. 1985. Peroxidation of linolenic acid promoted by human polymorphonuclear leucocytes. *J. Free Radic. Biol. Med.* **1**: 255–261.
41. Karnes, H. T., and C. March. 1993. Precision, accuracy, and data acceptance criteria in biopharmaceutical analysis. *Pharm. Res.* **10**: 1420–1426.
42. Jira, W., G. Spiteller, and A. Richter. 1998. Increased levels of lipid oxidation products in rheumatically destructed bones of patients suffering from rheumatoid arthritis. *Z. Naturforsch.* **53**: 1061–1071.
43. Ozawa, T., M. Hayakawa, K. Kosaka, S. Sugiyama, T. Ogawa, K. Yokoo, H. Aoyama, and Y. Izawa. 1990. Leukotoxin, 9,10-epoxy-12-ocaddecenoate, as a burn toxin causing adult respiratory distress syndrome. *Adv. Prostaglandin Thromboxane Leukot. Res.* **21**: 569–572.

44. Nithipatikom, K., A. J. Grall, B. B. Holmes, D. R. Harder, J. R. Falck, and W. B. Campbell. 2001. Liquid chromatographic-electrospray ionization-mass spectrometric analysis of cytochrome P450 metabolites of arachidonic acid. *Anal. Biochem.* **298**: 327–336.
45. Nithipatikom, K., P. F. Pratt, and W. B. Campbell. 2000. Determination of EETs using microbore liquid chromatography with fluorescence detection. *Am. J. Physiol. Heart Circ. Physiol.* **279**: H857–862.
46. Turk, J., B. A. Wolf, P. G. Comens, J. Colca, B. Jakschik, and M. L. McDaniel. 1985. Arachidonic acid metabolism in isolated pancreatic islets. IV. Negative ion-mass spectrometric quantitation of monooxygenase product synthesis by liver and islets. *Biochim. Biophys. Acta.* **835**: 1–17.
47. Kiprov, D. 1980. Experimental models of hypertension. *Cor Vasa.* **22**: 116–128.
48. Folkow, B., and G. Karlstrom. 1984. Age- and pressure-dependent changes of systemic resistance vessels concerning the relationships between geometric design, wall distensibility, vascular reactivity and smooth muscle sensitivity. *Acta Physiol. Scand.* **122**: 17–33.
49. Yu, Z., F. Xu, L. M. Huse, C. Morisseau, A. J. Draper, J. W. Newman, C. Parker, L. Graham, M. M. Engler, B. D. Hammock, D. C. Zeldin, and D. L. Kroetz. 2000. Soluble epoxide hydrolase regulates hydrolysis of vasoactive epoxyeicosatrienoic acids. *Circ. Res.* **87**: 992–998.
50. Schwartzman, M. L., J. R. Falck, P. Yadagiri, and B. Escalante. 1989. Metabolism of 20-hydroxyeicosatetraenoic acid by cyclooxygenase. Formation and identification of novel endothelium-dependent vasoconstrictor metabolites. *J. Biol. Chem.* **264**: 11658–11662.
51. Omata, K., N. G. Abraham, B. Escalante, and M. L. Schwartzman. 1992. Age-related changes in renal cytochrome P-450 arachidonic acid metabolism in spontaneously hypertensive rats. *Am. J. Physiol.* **262**: F8–16.
52. Yu, Z., L. M. Huse, P. Adler, L. Graham, J. Ma, D. C. Zeldin, and D. L. Kroetz. 2000. Increased CYP2J expression and epoxyeicosatrienoic acid formation in spontaneously hypertensive rat kidney. *Mol. Pharmacol.* **57**: 1011–1020.
53. Nakamura, T., D. L. Bratton, and R. C. Murphy. 1997. Analysis of epoxyeicosatrienoic and monohydroxyeicosatetraenoic acids esterified to phospholipids in human red blood cells by electrospray tandem mass spectrometry. *J. Mass Spectrom.* **32**: 888–896.